2015 IEEE 54th Annual Conference on Decision and Control (CDC)
December 15-18, 2015. Osaka, Japan

Design of Optimal Coupling Gains for Synchronization of Nonlinear Oscillators

Victor Purba, Xiaofan Wu, Mohit Sinha, Sairaj V. Dhople, and Mihailo R. Jovanović

Abstract— **This paper develops a structured optimal-control framework to design coupling gains for synchronization of weakly nonlinear oscillator circuits connected in resistive networks with arbitrary topologies. The oscillators are modeled as weakly nonlinear Liénard-type circuits, and the coupling gain amounts to the current gain which scales the output current of the oscillator. The structured optimal-control problem allows us to seek a decentralized control strategy (equivalently, a diagonal feedback matrix) that precludes communications between oscillators. To this end, a sparsity-promoting optimal control algorithm is developed to tune the optimal diagonal feedback-gain matrix with minimal performance sacrifice. This involves solving an $\mathcal{H}_2$ optimal control problem with ℓ_1 regularization by applying the alternating direction method of multipliers (ADMM). Simulation studies with application to voltage regulation in islanded networks composed of power-electronic inverters are provided to validate the approach.**

Index Terms— **Alternating direction method of multipliers, sparsity-promoting optimal control, synchronization, weakly nonlinear oscillators.**

I. Introduction

Synchronization of coupled Liénard-type oscillators is relevant to several engineering applications [1], [2]. This paper outlines a structured control-synthesis method to regulate the voltage amplitudes of a class of weakly nonlinear Liénard-type oscillators coupled through connected resistive networks with arbitrary topologies. The feedback gain takes the connotation of a current gain (which scales the output current of the oscillator); and the structured optimal-control problem is of interest since we seek a decentralized control strategy that precludes communications between oscillators. The problem setup is motivated by the application of controlling power-electronic inverters in low-inertia microgrids in the absence of conventional synchronous generators. A compelling time-domain approach to achieve a stable power system in this setting is to regulate the inverters to emulate the dynamics of weakly nonlinear limit-cycle oscillators which achieves network-wide synchrony in the absence of external forcing or any communication [3], [4]. That said, this paper offers several broad contributions to the topic of synchronization of nonlinear dynamical systems coupled over complex networks. First, we outline the control-synthesis approach with a broad level of generality to cover a wide array of circuit applications; in addition to power-systems and microgrids, these include solid-state circuit oscillators, semiconductor laser arrays, and microwave oscillator arrays [2], [5], [6]. Second, majority of the synchronization literature is primarily focused on phase- or pulse-coupled oscillator models [6], [7]. We depart from this line of work and focus on the complementary problem of optimally regulating the amplitude dynamics. (For the class of networks we study, phase synchrony can be guaranteed under fairly mild assumptions.)

Circuits with voltage dynamics governed by Liénard's equation are common in several applications [8]–[10]. (The ubiquitous Van der Pol oscillator is a particular example.) We study the setting where the oscillators are connected to a resistive network with an arbitrary topology. The oscillator output currents are scaled by a gain which assumes the focus of the control design. Designing coupling gains with a view to synchronize the outputs of dynamical systems has been studied in a variety of applications [11]–[13]. The nonlinear dynamics complicate our problem setting, and the solution strategy we propose draws from a variety of circuit- and system-theoretic tools including averaging methods for periodic nonlinear systems and structural reduction of electrical networks. Furthermore, conventional optimal control synthesis methods cannot guarantee decentralized control strategies (translating to local current gains). To address this, we leverage recent advances in structured control design.

Conventional optimal control design strategies typically return full feedback gain matrices. (A full feedback gain matrix in our setting would imply that extraneous communication links are required between the oscillators.) Since we seek a decentralized control strategy so that voltage regulation can be guaranteed only by tuning the local current gains, we leverage our expertise in structured feedback gain design for distributed systems that has demonstrated its effectiveness in the domain of power networks [14]–[18]. In particular, we present a sparsity-promoting optimal control design strategy [19] to design the current gains so that the differences between the oscillator terminal-voltage amplitudes can be minimized. The objective of the optimization problem is to tune the current gains to minimize the $\mathcal{H}_2$ norm of the system. In general, the optimization problem is non-convex and difficult to solve. We utilize the alternating direction method of multipliers (ADMM) algorithm to perform an iterative search for the optimal solution.

The control design strategy outlined above is tailored to linear system descriptions. The oscillator dynamics that derive from circuit laws are innately nonlinear and in Cartesian coordinates. As such, they pose a challenge for control synthesis. To facilitate control design, we leverage polar-

Support from the University of Minnesota Informatics Institute Transdisciplinary Faculty Fellowship; the National Science Foundation under awards ECCS-1407958, ECCS-1509277, CAREER award ECCS-1453921; and Minnesota's Discovery, Research and Innovation Economy grant are gratefully acknowledged.

The authors are with the Department of Electrical and Computer Engineering, University of Minnesota, Minneapolis, MN 55455. E-mails: {purba002, wuxxx836, sinha052, sdhople, mihailo}@umn.edu.

coordinate transformations, tools from averaging theory, and linear systems theory [1], [20]. First, by transforming the system into the polar coordinates, we extract the amplitude and phase dynamics of the terminal voltages. We then average the periodic dynamics and linearize the system around the nominal operating point.

The remainder of this paper is organized as follows. In Section II, we introduce the models for the oscillators and the resistive electrical network, and develop a coordinate transformation to represent the system in a standard state-space form. In Section III, we formulate the optimization problem to minimize the $\mathcal{H}_2$ norm of the system with a decentralized control scheme. In Section IV, we provide illustrative case studies to validate the approach. Concluding remarks and directions for future work are in Section V.

II. System of Coupled Weakly Nonlinear Oscillator Circuits

We begin this section with a description of the oscillator dynamics, and then describe the network interactions.

A. Nonlinear Oscillator Model

The oscillator dynamics are governed by

$$\ddot{v} + \varepsilon\, f(v)\dot{v} + \omega^2 v = \kappa\, \varepsilon\, \omega \dot{u}(t)\,, \tag{1}$$

where v is the terminal voltage, u is the input current, κ is the *current gain* (interchangeably referred as the *coupling gain*), ε is a positive real constant, and ω is the frequency of the voltage waveform for the unforced ($u = 0$) system in the so-called *quasi-harmonic* limit $\varepsilon \searrow 0$ [20]. All subsequent discussions assume operation in this quasi-harmonic limit since the terminal-voltage dynamics in this limit are approximately sinusoidal [20]. Function $f : \mathbb{R} \to \mathbb{R}$ satisfies the conditions in Liénard's theorem [2] for existence of a unique and stable limit cycle, in particular,

(A1) $f(v)$ is continuously differentiable $\forall v$.
(A2) $f(v)$ is an even function, i.e., $f(v) = f(-v), \forall v$.
(A3) Function $F(v) := \int_0^v f(z)dz$ has exactly one positive zero at $v = v_0$, is negative for $0 < v < v_0$, is positive and nondecreasing $\forall v > v_0$, and $\lim_{v\to\infty} F(v) \to \infty$.

Examples of nonlinear circuits that admit terminal-voltage dynamics of the form (1) include the ubiquitous Van der Pol oscillator (see Fig. 1 for more details), the dead-zone oscillator [3], a class of operational transconductance amplifiers [10], and dynamic translinear oscillator circuits [9].

To extract the amplitude and phase dynamics from (1), we seek a dynamical system representation in polar coordinates. To this end, define the change of variables $v = r\cos(\phi)$, $\omega \int_0^t v\, dt = r\sin(\phi)$, where r denotes the radius of the oscillator limit cycle, and ϕ represents the instantaneous phase of the resulting oscillations. It is straightforward to show that with this change of coordinates, we recover the following model:

$$\begin{aligned}\dot{r} &= \varepsilon(h(r\cos\phi) + \kappa\omega u(t))\cos\phi,\\ \dot{\phi} &= \omega - \left(\frac{\varepsilon}{r}h(r\cos\phi) - \varepsilon\kappa\omega\frac{u(t)}{r}\right)\sin\phi,\end{aligned} \tag{2}$$

where $h(z) := \int f(z)dz$. In subsequent developments, we will find it useful to work with the following model:

$$\begin{aligned}\dot{r} &= \varepsilon(h(r\cos(\omega t+\theta)) + \kappa\omega u(t))\cos(\omega t+\theta),\\ \dot{\theta} &= -\frac{\varepsilon}{r}\left(h(r\cos(\omega t+\theta)) + \kappa\,\omega u(t)\right)\sin(\omega t+\theta).\end{aligned} \tag{3}$$

where we define $\theta(t) := \phi(t) - \omega t$, with θ representing the phase offset with respect to the rotating reference frame of frequency ω. Since the system (3) is non-autonomous but periodic in t, we leverage averaging methods to obtain an autonomous system which admits similar dynamics [20]. In particular, for small values of ε we can average the periodic vector fields in (3) to obtain the so-called *slow flow* equations which are accurate up to $\mathcal{O}(\varepsilon)$ [21].

Let us denote $\overline{r}$ and $\overline{\theta}$ to be the $2\pi/\omega$-averaged values of the periodic signals r and θ, respectively. In the quasi-harmonic limit, i.e., $\varepsilon \searrow 0$, we apply standard averaging arguments using ε as the *small parameter*, to obtain the averaged dynamics [20, Theorem 10.4] [1], [22]

$$\begin{aligned}\begin{bmatrix}\dot{\overline{r}}\\ \dot{\overline{\theta}}\end{bmatrix} &= \frac{\varepsilon\omega}{2\pi}\int_0^{2\pi/\omega}\begin{bmatrix} h(\overline{r}\cos(\omega t+\overline{\theta}))\cos(\omega t+\overline{\theta})\\ -\frac{1}{\overline{r}}h(\overline{r}\cos(\omega t+\overline{\theta}))\sin(\omega t+\overline{\theta})\end{bmatrix}dt\\ &\quad + \frac{\varepsilon\kappa\omega^2}{2\pi}\int_0^{2\pi/\omega}\begin{bmatrix} u(t)\cos(\omega t+\overline{\theta})\\ -\frac{1}{\overline{r}}u(t)\sin(\omega t+\overline{\theta})\end{bmatrix}dt\\ &= \frac{\varepsilon}{2\pi}\begin{bmatrix} -\overline{f}(\overline{r}) + \kappa\omega^2\int_0^{\frac{2\pi}{\omega}} u(t)\cos(\omega t+\overline{\theta})dt\\ -\kappa\omega^2\int_0^{\frac{2\pi}{\omega}}\frac{u(t)}{\overline{r}}\sin(\omega t+\overline{\theta})dt\end{bmatrix},\end{aligned} \tag{4}$$

where

$$\overline{f}(\overline{r}) := 4\int_0^{\overline{r}} f(\sigma)\sqrt{1-\frac{\sigma^2}{\overline{r}^2}}\,d\sigma. \tag{5}$$

B. Resistive Electrical Network

We consider a collection of N oscillators with dynamics of the form (1) (or equivalently, (4)) connected in a resistive electrical network. The oscillators are assumed to be identical in all aspects except for the current gains. The nodes of the resistive electrical network are collected in the set $\mathcal{A}$, and branches (edges) are collected in the set $\mathcal{E} := \{(j,\ell)\} \subset \mathcal{A}\times\mathcal{A}$. Let $\mathcal{N} := \{1,\dots,N\} \subseteq \mathcal{A}$ denote nodes that the oscillators are connected to, and denote the set of *internal nodes* as $\mathcal{I} := \mathcal{A}\setminus\mathcal{N}$. Shunt loads—also modeled as resistances—are connected to the internal nodes $\mathcal{I}$. Denote the vectors that collect the nodal current injections and node voltages in the network by $i_{\mathcal{A}}$ and $v_{\mathcal{A}}$, respectively. Note that since the network is resistive, $i_{\mathcal{A}}$ and $v_{\mathcal{A}}$ are real-valued functions of time. The electrical coupling between

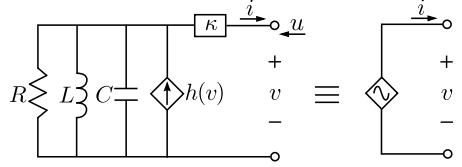

Fig. 1: The Van der Pol oscillator circuit with a current gain κ admits the dynamics in (1). In this case, $\omega = 1/\sqrt{LC}$, $\varepsilon = \sqrt{L/C}$, and $h(v) = \int f(v)dv = \alpha\omega(v - \beta v^3/3)$ where α and β are positive real constants.

the oscillators is described by Kirchhoff's and Ohm's laws, which read in matrix-vector form as

$$i_{\mathcal{A}} = G_{\mathcal{A}} v_{\mathcal{A}}, \tag{6}$$

with entries of the *conductance matrix* $G_{\mathcal{A}}$ given by

$$[G_{\mathcal{A}}]_{j\ell} := \begin{cases} g_j + \sum_{(j,k)\in\mathcal{E}} g_{jk}, & \text{if } j = \ell, \\ -g_{j\ell}, & \text{if } (j,\ell) \in \mathcal{E}, \\ 0, & \text{otherwise}, \end{cases} \tag{7}$$

with $g_j \in \mathbb{R}_{\geq 0}$ denoting the shunt conductance at node j, and $g_{j\ell} = g_{\ell j} \in \mathbb{R}_{\geq 0}$ the conductance of the line (j,ℓ).

Let $i = [i_1, \ldots, i_N]^{\mathrm{T}}$ and $v = [v_1, \ldots, v_N]^{\mathrm{T}}$ be the vectors of inverter current injections and terminal voltages, respectively, and let $i_{\mathcal{I}}$ and $v_{\mathcal{I}}$ be the vectors collecting the current injections and nodal voltages for the interior nodes. Note that entries of $i_{\mathcal{I}}$ are zero. With this notation in place, we can rewrite (6) as

$$\begin{bmatrix} i \\ 0 \end{bmatrix} = \begin{bmatrix} G_{\mathcal{N}\mathcal{N}} & G_{\mathcal{N}\mathcal{I}} \\ G_{\mathcal{N}\mathcal{I}}^{\mathrm{T}} & G_{\mathcal{I}\mathcal{I}} \end{bmatrix} \begin{bmatrix} v \\ v_{\mathcal{I}} \end{bmatrix}. \tag{8}$$

For the resistive networks we consider in this work, $G_{\mathcal{I}\mathcal{I}}$ is always nonsingular due to irreducible diagonal dominance [23]. Therefore, the second set of equations in (8) can be uniquely solved for the interior voltages, $v_{\mathcal{I}}$. Then, we obtain the following equations relating the oscillator current injections and terminal voltages:

$$i = \left(G_{\mathcal{N}\mathcal{N}} - G_{\mathcal{N}\mathcal{I}} G_{\mathcal{I}\mathcal{I}}^{-1} G_{\mathcal{N}\mathcal{I}}^{\mathrm{T}}\right) v =: Gv. \tag{9}$$

We refer to the matrix G in (9) as the *Kron-reduced conductance matrix* and this model reduction through a Schur complement of the conductance matrix is known as *Kron reduction* [23]. Notice that the entries of G define the effective electrical conductances between the oscillators in the network, as well as the effective local resistive loads for each oscillator. An illustration of Kron reduction for a network with three oscillators is shown in Fig. 2. Under some mild assumptions on the originating network, it follows that the Kron-reduced network is fully connected [23].

With a slight abuse of notation, we denote the effective shunt-conductance load for the jth oscillator by g_j, and the effective conductance of the (j,ℓ) line in the Kron-reduced electrical network by $g_{j\ell}$ in all subsequent discussions. Also, we will find it useful to define $g_{jj} := g_j + \sum_{k=1,k\neq j}^{N} g_{jk}$.

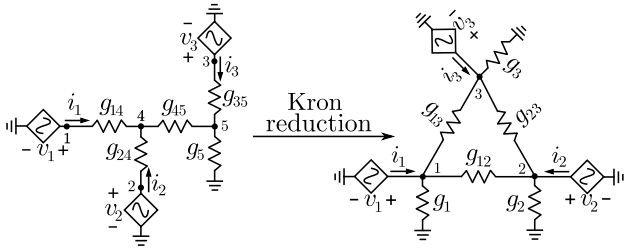

Fig. 2: Kron reduction illustrated for a network of three oscillators. In this example, $\mathcal{A} = \{1, \ldots, 5\}$, $\mathcal{N} = \{1, 2, 3\}$, and $\mathcal{I} = \{4, 5\}$.

C. System Dynamical Model in Polar Coordinates

With this notation in place, for the resistive network, the current input for the jth oscillator, $u_j(t)$ is given by:

$$u_j(t) = -i_j(t) = -\sum_{\ell=1}^{N} g_{j\ell} \overline{r}_\ell \cos(\omega t + \overline{\theta}_\ell). \tag{10}$$

Substituting (10) in (4), and denoting $\overline{\theta}_{j\ell} = \overline{\theta}_j - \overline{\theta}_\ell$, we get the following polar-coordinates representation for the dynamics of the jth oscillator:

$$\frac{d\overline{r}_j}{dt} = -\frac{\varepsilon \overline{f}(\overline{r}_j)}{2\pi} - \frac{\kappa_j \varepsilon \omega}{2} g_{jj} \overline{r}_j + \frac{\kappa_j \varepsilon \omega}{2} \sum_{\ell=1,\ell\neq j}^{N} g_{j\ell} \overline{r}_\ell \cos(\overline{\theta}_{j\ell}), \tag{11a}$$

$$\frac{d\overline{\theta}_j}{dt} = -\frac{\kappa_j \varepsilon \omega}{2\overline{r}_j} \sum_{\ell=1,\ell\neq j}^{N} g_{j\ell} \overline{r}_\ell \sin(\overline{\theta}_{j\ell}). \tag{11b}$$

D. State-space representation of linearized system

Our objective is to design an optimal set of coupling gains, $\kappa_1, \ldots, \kappa_N$, that ensure the terminal voltages of the nonlinear oscillator dynamics in (11) are regulated to a common value. For the class of oscillator models we consider, it is known that there exists a unique and stable limit cycle with radius $\overline{r}_{\mathrm{eq}}$ which satisfies $\overline{f}(\overline{r}_{\mathrm{eq}}) = 0$ [2]. With a view towards leveraging control design techniques from linear systems theory, we linearize the system around $(\overline{r}_{\mathrm{eq}} 1_N, \overline{\theta}_{\mathrm{eq}})$ (where 1_N denotes $N \times 1$ vector of all ones); $\overline{\theta}_{\mathrm{eq}}$ is the phase-synchronized equilibrium (we comment on it next). The Jacobian of the system around the equilibrium point can be partitioned into blocks as follows:

$$J = \left[\begin{array}{c|c} J_{\mathrm{A}} & J_{\mathrm{B}} \\ \hline J_{\mathrm{C}} & J_{\mathrm{D}} \end{array}\right]. \tag{12}$$

The entries of J_{A}, J_{B}, J_{C}, and J_{D} are specified as:

$$\begin{aligned}
\left[J_{\mathrm{A}}\right]_{j\ell} &= \begin{cases} -\frac{\varepsilon}{2\pi} f'(\overline{r}_{\mathrm{eq}}) - \kappa_j \frac{\varepsilon\omega}{2} g_{jj} & \text{if } j = \ell \\ \kappa_j \frac{\varepsilon\omega}{2} g_{jl} \cos(\overline{\theta}_{\mathrm{eq},j\ell}) & \text{if } j \neq \ell \end{cases} \\
\left[J_{\mathrm{B}}\right]_{j\ell} &= -\kappa_j \tfrac{\varepsilon\omega}{2} g_{j\ell} \overline{r}_{\mathrm{eq}} \sin(\overline{\theta}_{\mathrm{eq},j\ell}) \\
\left[J_{\mathrm{C}}\right]_{j\ell} &= \begin{cases} \kappa_j \frac{\varepsilon\omega}{2\overline{r}_{\mathrm{eq}}^2} \sum_{\ell=1,\ell\neq j}^{N} g_{j\ell} \sin(\overline{\theta}_{\mathrm{eq},j\ell}) & \text{if } j = \ell \\ -\kappa_j \frac{\varepsilon\omega}{2} g_{j\ell} \sin(\overline{\theta}_{\mathrm{eq},j\ell}) & \text{if } j \neq \ell \end{cases} \\
\left[J_{\mathrm{D}}\right]_{j\ell} &= \begin{cases} -\kappa_j \frac{\varepsilon\omega}{2} \sum_{\ell=1,\ell\neq j}^{N} g_{j\ell} \cos(\overline{\theta}_{\mathrm{eq},j\ell}) & \text{if } j = \ell \\ \kappa_j \frac{\varepsilon\omega}{2} g_{j\ell} \cos(\overline{\theta}_{\mathrm{eq},j\ell}) & \text{if } j \neq \ell \end{cases},
\end{aligned}$$

where $f'(\overline{r}_{\mathrm{eq}})$ represents the derivative of $\overline{f}(\cdot)$ evaluated at $\overline{r}_{\mathrm{eq}}$. An inspection of the above Jacobian reveals that the phase-synchronized equilibrium i.e., $\overline{\theta}_{\mathrm{eq},j} = \overline{\theta}_{\mathrm{eq},\ell}\, \forall j, \ell$, is locally exponentially stable. First, notice that J is block diagonal for this equilibrium and therefore around this equilibrium, the evolution of amplitudes and phases are *decoupled*. Furthermore, J_{A} and J_{D} are diagonally dominant symmetric matrices (which implies that they are negative semi-definite and therefore overall J is negative semi-definite), leveraging LaSalle's invariance principle it can be shown that phase synchronized equilibrium is locally exponentially stable [24,

Theorem 4.3]. With these arguments in place, we proceed with the linearized (and decoupled) amplitude dynamics.

For small perturbations about the equilibrium point, we express $\overline{r} = \overline{1}_N r_{\rm eq} + \widetilde{r}$, where $\widetilde{r} := [\widetilde{r}_1\ \widetilde{r}_2\ \cdots\ \widetilde{r}_N]^{\rm T}$. By defining states $x = \widetilde{r}$, the linearized system can be written in the state-space model

$$\begin{aligned}\dot{x} &= \widehat{A}\,x\ +\ u\ +\ \widehat{B}\,d \\ &= -\left(\frac{\varepsilon}{2\pi}\,\overline{f}'(\overline{r}_{\rm eq})I_N\ +\ \frac{\varepsilon\omega}{2}K_{\rm d}\,G\right)\,x\ +\ \widehat{B}\,d \end{aligned} \tag{13}$$

where I_N is the $N \times N$ identity; $\widehat{A} = -\frac{\varepsilon}{2\pi}\overline{f}'(\overline{r}_{\rm eq})I_N$; the control input, $u = -\frac{\varepsilon\omega}{2}K_{\rm d}Gx$ (with a slight abuse of notation with regard to (1)); and $\widehat{B}$ is the input matrix for external disturbances d. Recall that G is the Kron-reduced conductance matrix, and $K_{\rm d} = {\rm diag}\{\kappa_1, \ldots, \kappa_N\}$. With regard to control synthesis, $K_{\rm d}$ takes the connotation of the feedback-gain matrix. In general, $\widehat{B}$ can be chosen according to the application; and in this particular case, we make the choice $\widehat{B} = G$. With due regard to the optimal control problem to be formulated in Section III, we define the vector of performance outputs, z, as follows:

$$z = \left[\begin{array}{c} \widehat{Q}^{1/2} \\ -\widehat{R}^{1/2}\,K_{\rm d}\,G \end{array}\right] x, \tag{14}$$

where $\widehat{Q}$ is the state penalty matrix; and $\widehat{R}$ is the control input penalty matrix.

A cursory inspection of (13)-(14) indicates two impediments in applying conventional linear feedback control design approaches: i) the closed-loop system is not in standard feedback control form, (the standard form would be $\dot{x} = (\widehat{A} - GK)x + \widehat{B}d$); ii) there is a structural constraint on the feedback gain matrix, K, being diagonal (of the form $K_{\rm d}$). To reformulate the problem so that conventional linear feedback control design approaches can be used, we first introduce a change of variables, $\psi = Gx$. Note that G is invertible when the network has shunt loads [25]. The state-space model for the system in these new coordinates can be expressed in the following form:

$$\begin{aligned}\dot{\psi}\ &=\ (A\ -\ G\,K_{\rm d})\,\psi\ +\ B\,d \\ \xi\ &=\ \left[\begin{array}{c} Q^{1/2} \\ -R^{1/2}\,K_{\rm d} \end{array}\right]\psi, \end{aligned} \tag{15}$$

where

$$\begin{aligned} A\ &=\ G\,\widehat{A}\,G^{-1}, \qquad B\ =\ G\,\widehat{B} \\ Q\ &=\ G^{-1}\,\widehat{Q}\,G^{-1}, \quad R\ =\ \widehat{R}. \end{aligned}$$

Next, we introduce an optimal control design method that will allow us to synthesize a diagonal feedback gain matrix.

III. Design of Current Gains

In this section, we introduce a sparsity-promoting optimal control algorithm developed in [16], [19] to synthesize optimal current gains for the oscillators with the objective of regulating their terminal voltages to a common value.

A. Linear quadratic control design

We cast the task of synthesizing the current gains as an optimal feedback control design problem. With reference to (15), we select the state penalty matrix $\widehat{Q} = I_N$ to ensure that the terminal-voltage amplitudes of all circuits coincide. Furthermore, we set the control input penalty matrix $\widehat{R} = \rho I_N$, $\rho \in \mathbb{R}^+$. The closed-loop $\mathcal{H}_2$ norm from input disturbance d to performance output z is defined as

$$J(K)\ :=\ \begin{cases} {\rm trace}\left(B^{\rm T}\,P(K)\,B\right) & K \text{ stabilizing} \\ \infty & \text{otherwise,} \end{cases} \tag{16}$$

where the closed-loop observability Gramian $P(K)$ satisfies the Lyapunov equation

$$(A - G\,K)^{\rm T}P + P\,(A - G\,K)\ =\ -(Q + K^{\rm T}R\,K), \tag{17}$$

and K is the feedback-gain matrix. Conventional $\mathcal{H}_2$ control design methods, such as the Linear Quadratic Regulator (LQR) problem, provide us with an optimal centralized controller. In our problem setting, dense feedback gain matrices require communication links to relay information about oscillator currents. However, we want to ensure that the feedback matrix is diagonal so that each oscillator only requires local current measurements. Next, we introduce the sparsity-promoting optimal control algorithm to incorporate the structure constraint on the feedback matrix K to get a fully diagonal matrix $K_{\rm d}$.

B. Sparsity-promoting optimal control

Consider the following optimization problem:

$$\begin{array}{ll} \text{minimize} & J(K)\ +\ \gamma\,g(F) \\ \text{subject to} & K\ -\ F\ =\ 0, \end{array} \tag{18}$$

where $J(K)$ is defined in (16), $g(F)$ is the sparsity-promoting penalty function, and γ is the emphasis on sparsity. When γ is zero, objective function (18) only minimizes $J(K)$, which provides us with the optimal centralized controller. As γ increases, the emphasis on the sparsity penalty function increases, so we obtain sparser feedback-gain matrices, at the expense of system performance. See Fig. 3 for an illustration. By decoupling the objective functions J and g

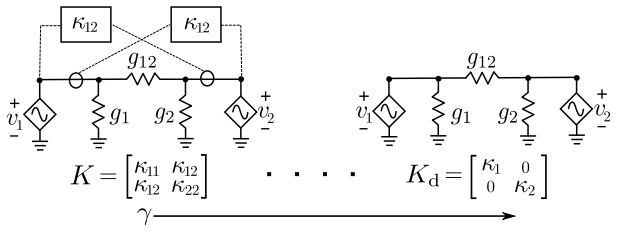

Fig. 3: Sparsity-promoting optimal current gain design illustrated for a Kron-reduced network and two oscillators. As the sparsity emphasis γ increases, K becomes sparser and we eventually recover a diagonal matrix, $K_{\rm d}$, which corresponds to local current gains. Dotted lines indicate communication links that correspond to dense feedback gain matrices.

and introducing the linear constraint $K - F = 0$ in (18), the alternating direction method of multipliers (ADMM) algorithm suggests a solution approach by exploiting the separability of g and differentiability of J; see [16], [19] for the details of the algorithm. The penalty function $g(F)$ is determined by a weighted ℓ_1 norm [19]:

$$g(F) \;:=\; \sum_{i,\,j} W_{ij}\,|F_{ij}|, \tag{19}$$

where $W_{ij} = 1/(|F_{ij}| + \epsilon)$ are positive weights, see [26] for detailed procedure of selecting W_{ij}'s.

The algorithm consists of the following steps: First, we form the augmented Lagrangian; then we use ADMM for the augmented Lagrangian minimization, which includes a K-minimization step, an F-minimization step, and a dual-variable update step. ADMM identifies a specific sparsity pattern and provides a good initial condition for the structured feedback design. Finally, we implement a polishing step, which involves solving a structured $\mathcal{H}_2$ problem for the fixed controller structure. Since the optimization problem (18) is non-convex in general, the sparsity-promoting optimal control algorithm would only guarantee local optimal solutions. Readers are referred to [16], [19] for further information.

IV. Case Studies

To verify the effectiveness of our algorithm for optimal current-gain design, we test it on a resistive network with the same topology as the IEEE 37-bus benchmark network and a collection of $N = 7$ Van der Pol oscillators (see Fig. 6 for the network topology). The dynamics of the oscillators can be described using (1) with $f(v) = \alpha\omega(1 - \beta v^2)$, where α and β are positive constants. (See Fig. 1 for a detailed circuit schematic). It follows from (11) that the averaged voltage-amplitude dynamics of the jth oscillator are:

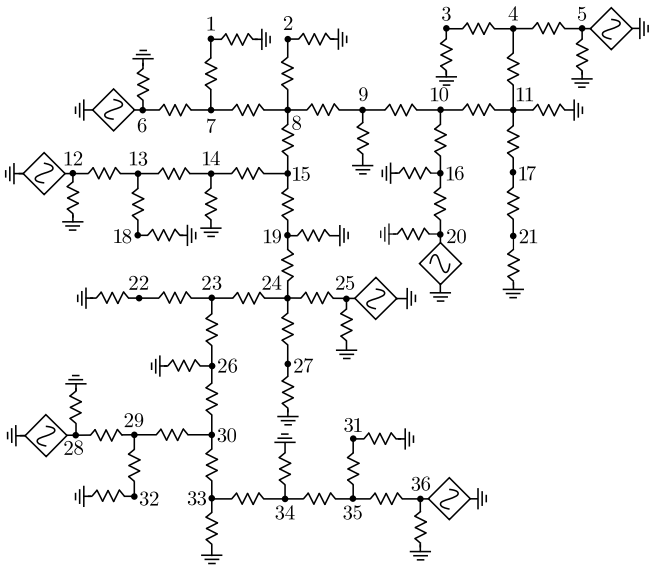

Fig. 4: Schematic diagram of the electrical network. The topology is adopted from the IEEE 37-bus network.

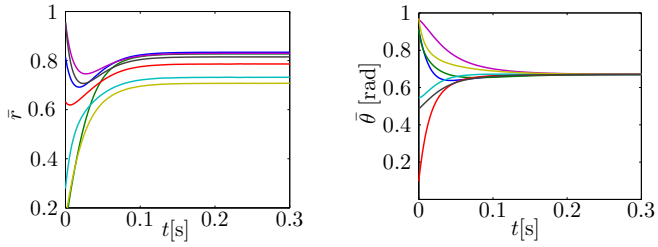

Fig. 5: Evolution of averaged amplitudes and phases with time for the nonlinear system in (11).

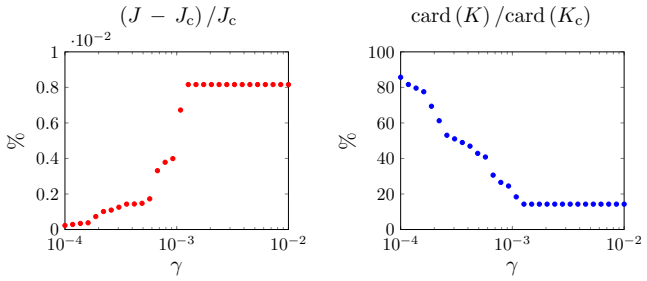

Fig. 6: Performance versus sparsity comparison of sparse K and the optimal centralized controller K_c.

$$\frac{d}{dt}\overline{r}_j = -\varepsilon\alpha\omega\left(-\frac{1}{2}\overline{r}_j + \frac{\beta}{8}\overline{r}_j^3\right) - \frac{\kappa_j\varepsilon\omega}{2}g_{jj}\overline{r}_j + \frac{\kappa_j\varepsilon\omega}{2}\sum_{\ell=1,\ell\neq j}^{N} g_{j\ell}\overline{r}_\ell\cos(\overline{\theta}_{j\ell}). \tag{20}$$

Linearizing (20) around the stable equilibrium point of the decoupled oscillator, $\overline{r}_{\rm eq} = 2/\sqrt{\beta}$ [20], and acknowledging that the phase-synchronized equilibrium is locally exponentially stable, we recover the state-space model of the form (13) with $\widehat{A} = -\varepsilon\alpha\omega I_N$.

For the simulations that follow, we pick $\alpha = 0.90$, $\beta = 4$, $\omega = 2\pi 60\,\mathrm{rad/s}$, $\varepsilon = 0.19$; conductances of the lines in the IEEE-37-bus network are sourced from [27].

Fig. 5 shows the averaged voltage magnitude and phase trajectories of all seven oscillators when we apply unit current gains (without control design) to the original nonlinear coupled system (11). It is evident that the terminal-voltage magnitudes do not synchronize as time evolves but the phases synchronize innately.

A. Optimal current-gain design

The sparsity-promoting optimal control problem in (18) is solved with 30 logarithmically-spaced points for $\gamma \in [10^{-4}, 10^{-2}]$. In Fig. 6, we can see that as emphasis on sparsity increases, the number of nonzero elements in the feedback matrix—returned by the cardinality function $\mathrm{card}(.)$—reduces. For $\gamma = 10^{-2}$, the sparsity-promoting optimal control algorithm returns a diagonal feedback controller, K_d with diagonal entries: $\kappa_1 = 0.0033$, $\kappa_2 = 0.0047$, $\kappa_3 = 0.0026$, $\kappa_4 = 0.0025$, $\kappa_5 = 0.0047$, $\kappa_6 = 0.0038$, $\kappa_7 = 0.0029$. With this fully decentralized controller, we

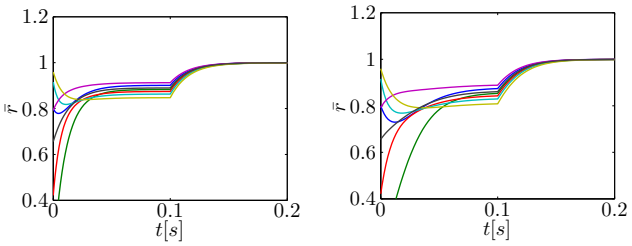

(a) Linearized system (b) Nonlinear system

Fig. 7: Oscillator terminal-voltage magnitudes with designed current gains applied at time $t = 0.1\,\mathrm{s}$.

drop 80% of the nonzero elements in the feedback matrix compared to the optimal centralized controller (denoted by K_{c} with corresponding cost J_{c}), at the expense of only 0.01% performance loss.

B. Time-domain Simulations for Original Nonlinear and Linearized Models

To demonstrate the efficacy of our control design method, we simulate both the linear model (15) and the original nonlinear model (20) for Van der pol oscillators, with the optimal κ's that are obtained from the sparsity-promoting optimal control algorithm. Fig. 7 shows the trajectories of the averaged terminal-voltage magnitudes for each inverter with optimal gains applied at time $t = 0.1\,\mathrm{s}$, with unit current gains as initial values. From the figure, it is clear that calibrating the current gains leads to synchronization of terminal voltage amplitudes. Furthermore, since the original nonlinear system also achieves amplitude synchronization, it validates our linearized design perspective.

V. Concluding Remarks

In this paper, we introduced a systematic way of designing current gains for weakly nonlinear circuits governed by Liénard's equation in a resistive electrical network. The output current of each oscillator is scaled by a current gain; and the objective is to synthesize an optimal set of current gains to ensure voltage regulation in the network. We apply a sparsity-promoting optimal control method to design the current gains. The optimization problem targets simultaneously achieving a desirable system performance and preserving the sparsity pattern, which is the diagonal structure of the feedback matrix. An iterative ADMM algorithm is used to solve the ℓ_1 regularized version of the standard $\mathcal{H}_2$ optimal control problem. Ongoing research is focused on extending the approach to cover networks with inductive and capacitive elements.

References

[1] S. E. Tuna, "Synchronization analysis of coupled lienard-type oscillators by averaging," *Automatica*, vol. 48, no. 8, pp. 1885–1891, 2012.

[2] S. H. Strogatz, *Nonlinear Dynamics and Chaos: With Applications to Physics, Biology, Chemistry, and Engineering*, 1st ed., ser. Studies in nonlinearity. Westview Press, Jan. 2001.

[3] B. B. Johnson, S. V. Dhople, A. O. Hamadeh, and P. T. Krein, "Synchronization of parallel single-phase inverters with virtual oscillator control," *IEEE Trans. Power Electron.*, vol. 29, no. 11, pp. 6124–6138, Nov. 2014.

[4] L. A. B. Tôrres, J. P. Hespanha, and J. Moehlis, "Power supplies dynamical synchronization without communication," in *Proc. of the Power & Energy Society 2012 General Meeting*, July 2012.

[5] K. Josić and S. Peleš, "Synchronization in networks of general, weakly nonlinear oscillators," *Journal of Physics A: Mathematical and General*, vol. 37, no. 49, p. 11801, 2004.

[6] F. Dörfler and F. Bullo, "Synchronization in complex networks of phase oscillators: A survey," *Automatica*, vol. 50, no. 6, pp. 1539–1564, 2014.

[7] A. Mauroy, P. Sacré, and R. J. Sepulchre, "Kick synchronization versus diffusive synchronization," in *IEEE Conference on Decision and Control*, 2012, pp. 7171–7183.

[8] T. Koga and M. Shinagawa, "An extension of the lienard theorem and its application [nonlinear circuits]," in *Circuits and Systems, 1991., IEEE International Sympoisum on*, Jun 1991, pp. 1244–1247 vol.2.

[9] W. A. Serdijn, J. Mulder, A. C. van der Woerd, and A. H. van Roermund, "A wide-tunable translinear second-order oscillator," *Solid-State Circuits, IEEE Journal of*, vol. 33, no. 2, pp. 195–201, 1998.

[10] K. Odame, "Exploiting device nonlinearity in analog circuit design," Ph.D. dissertation, Georgia Institute of Technology, 2008.

[11] P. De Lellis, M. di Bernardo, and F. Garofalo, "Synchronization of complex networks through local adaptive coupling," *Chaos: An Interdisciplinary Journal of Nonlinear Science*, vol. 18, no. 3, 2008.

[12] S. E. Tuna, "Lqr-based coupling gain for synchronization of linear systems," *arXiv preprint arXiv:0801.3390*, 2008.

[13] A. Hamadeh, G.-B. Stan, and J. Goncalves, "Constructive synchronization of networked feedback systems," in *IEEE Conference on Decision and Control*, December 2010, pp. 6710–6715.

[14] F. Dörfler, M. R. Jovanović, M. Chertkov, and F. Bullo, "Sparse and optimal wide-area damping control in power networks," in *Proceedings of the 2013 American Control Conference*, Washington, DC, 2013, pp. 4295–4300.

[15] F. Dörfler, M. R. Jovanović, M. Chertkov, and F. Bullo, "Sparsity-promoting optimal wide-area control of power networks," *IEEE Trans. Power Syst.*, vol. 29, no. 5, pp. 2281–2291, September 2014.

[16] X. Wu and M. R. Jovanović, "Sparsity-promoting optimal control of consensus and synchronization networks," in *Proceedings of the 2014 American Control Conference*, Portland, OR, 2014, pp. 2948–2953.

[17] X. Wu, F. Dörfler, and M. R. Jovanović, "Analysis and design trade-offs for power network inter-area oscillations," in *Proceedings of the 21st International Symposium on Mathematical Theory of Network and Systems*, Groningen, The Netherlands, 2014, pp. 657–663.

[18] X. Wu, F. Dörfler, and M. R. Jovanović, "Input-output analysis and decentralized optimal control of inter-area oscillations in power systems," *IEEE Trans. Power Syst.*, 2015, doi:10.1109/TPWRS.2015.2451592; also arXiv:1502.03221.

[19] F. Lin, M. Fardad, and M. R. Jovanović, "Design of optimal sparse feedback gains via the alternating direction method of multipliers," *IEEE Trans. Automat. Control*, vol. 58, no. 9, pp. 2426–2431, September 2013.

[20] H. K. Khalil, *Nonlinear Systems*, 3rd ed. Prentice Hall, 2002.

[21] R. H. Rand, "Lecture notes on nonlinear vibrations," 2012.

[22] M. Sinha, F. Dörfler, B. B. Johnson, and S. V. Dhople, "Uncovering droop control laws embedded within the nonlinear dynamics of van der pol oscillators," *IEEE Trans. Control of Networked Sys.*, 2014, in review.

[23] F. Dörfler and F. Bullo, "Kron reduction of graphs with applications to electrical networks," *IEEE Transactions on Circuits and Systems I: Regular Papers*, vol. 60, no. 1, pp. 150–163, Jan. 2013.

[24] F. Dörfler and F. Bullo, "Exploring synchronization in complex oscillator networks," *arXiv preprint arXiv:1209.1335*, 2012.

[25] S. V. Dhople, B. B. Johnson, F. Dorfler, and A. O. Hamadeh, "Synchronization of nonlinear circuits in dynamic electrical networks with general topologies," *Circuits and Systems I: Regular Papers, IEEE Transactions on*, vol. 61, no. 9, pp. 2677–2690, 2014.

[26] E. J. Candès, M. B. Wakin, and S. P. Boyd, "Enhancing sparsity by reweighted ℓ_1 minimization," *J. Fourier Anal. Appl*, vol. 14, pp. 877–905, 2008.

[27] L. Luo and S. Dhople, "Spatiotemporal model reduction of inverter-based islanded microgrids," *IEEE Transactions on Energy Conversion*, vol. 29, no. 4, pp. 823–832, Dec 2014.